Analyst

Ultrasensitive detection of acephate based on carbon quantum dots-mediated fluorescence inner filter effects

Journal:	*Analyst*
Manuscript ID	AN-ART-09-2022-001552.R1
Article Type:	Paper
Date Submitted by the Author:	25-Oct-2022
Complete List of Authors:	Li, Haiqin ; Taiyuan University of Technology, College of Biomedical Engineering Deng, Rong; Taiyuan University of Technology, College of Biomedical Engineering Tavakoli, Hamed; University of Texas at El Paso, Chemistry and Biochemistry Li, Xiaochun; Taiyuan University of Technology, Li, Xiujun; The University of Texas at El Paso, Chemistry

Ultrasensitive detection of acephate based on carbon quantum dots-mediated fluorescence inner filter effects

Haiqin Li,[†] Rong Deng,[†] Hamed Tavakoli,[‡] Xiaochun Li,[†,*] and XiuJun Li [‡,*]

[†] *Institute of Biomedical Precision Testing and Instrumentation, College of Biomedical Engineering, Taiyuan University of Technology, Jinzhong 030600, P.R. China*

[‡] *Department of Chemistry and Biochemistry, Forensic Science, & Environmental Science & Engineering, University of Texas at El Paso, 500 W University Ave, El Paso, Texas 79968, United States*

[*] Corresponding authors. lixiaochun@tyut.edu.cn (XC. Li); xli4@utep.edu (XJ. Li).

Abstract

Acephate is an organophosphorus pesticide (OPs) that is widely used to control insects in agricultural fields such as vegetables and fruits. Toxic OPs can enter human and animal bodies and eventually lead to chronic or acute poisoning. However, traditional enzyme inhibition and colorimetric methods for OPs detection usually require complicated detection procedures and prolonged time and have low detection sensitivity. High-sensitivity monitoring of trace levels of acephate residues is of great significance to food safety and human health. Here, we developed a simple method for ultrasensitive quantitative detection of acephate based on the carbon quantum dots (CQDs)-mediated fluorescence inner filter effect (IFE). In this method, the fluorescence from CQDs at 460 nm quenched by 2, 3-diaminophenazine (DAP) and the resulted fluorescence from DAP at 558 nm through an IFE mechanism between CQDs and DAP, form ratiometric responses. The ratiometric signal I_{558}/I_{460} was found to exhibit a linear relationship with the concentration of acephate. The detection limit of this method was 0.052 ppb, which is far lower than the standards for acephate from China and EU in food safety administration. The ratiometric fluorescent sensor was further validated by testing spiked samples of tap water and pear, indicating great potential for sensitive detection of trace OPs in complex matrixes of real samples.

Keywords： Acephate; Inner filter effect (IFE); Carbon quantum dots (CQDs); Enzyme inhibition; organophosphorus pesticides (OPs)

1. Introduction

In recent decades, organophosphorus pesticides (OPs) such as acephate have been widely used in the prevention, control and elimination of plant diseases and insect pests on vegetables and fruits [1, 2]. However, except approximately 2.5% of the pesticides for pest control, the remaining 97.5% is left in the soil, atmosphere, and water resources [3]. This eventually inhibits the activity of cholinesterase when it enters the human body directly or indirectly through bioconcentration, direct human contact, and eating, resulting in a large accumulation of the neurotransmitter acetylcholine (ATCh) [4]. As a consequence, the accumulated ATCh blocks nerve conduction, poisoning the central nervous system and harming human health [5]. This has become an increasing issue as the abuse of pesticides is currently a global concern. [6]. Therefore, maximum allowable limits of different OPs have been set by regulatory agencies. For instance, the maximum allowable limit of acephate in food is 0.02 ppm [7]. Hence, it is very important to accurately detect and quantify trace levels of pesticides in food and the environment.

A variety of well-developed technologies have been applied for the detection of OPs mainly including gas chromatography (GC) [8,9], high-performance liquid chromatography (HPLC) [10], and capillary electrophoresis [11]. Although they possess obvious advantages in detection accuracy, high throughput, and reproducibility, these methods require sophisticated and expensive detection instruments, and time-consuming and professional operations. Therefore, more rapid and low-cost biosensors have been explored for the quantitation of pesticides, mainly including enzyme-linked immunosorbent assays [12], electrochemical methods [13,14], enzyme inhibition combined with colorimetric analysis methods [15-18], and surface enhanced Raman scattering [19,20]. However, these methods still have shortcomings such as low sensitivity, requirements of high-affinity antibodies, and false-positive results (low specificity). Thus, there is an urgent need to develop new highly sensitive methods for the detection of OPs.

Due to high sensitivity, fast response, and high signal-to-noise ratios of fluorescence

[21,22], fluorescence-based biochemical sensors have been developed for OPs quantitation, including silicon quantum dots (SiQDs) [23], CdTe/ZnCdSe quantum dots [24], organic fluorescent dyes [25] and aggregation-induced luminescent molecules (AIE) [26]. However, most of these metal-based quantum dots or organic fluorescent molecules usually have poor water solubility, long preparation time, and toxicity, which lead to limited applications for food safety surveillance. Conversely, as a new type of carbon-based nanomaterials, carbon quantum dots (CQDs), possess many advantages such as tunable fluorescence emission dependent on size and excitation wavelength, ease of preparation [27], high stability, better water solubility, non-toxic and excellent biocompatibility [28]. Furthermore, compared with other fluorescence quenching mechanisms such as static quenching, dynamic quenching, photoinduced electron transfer (PET), and Förster resonance energy transfer (FRET), the fluorescence inner filter effect (IFE) can be readily used for CQDs-based fluorescence sensors without complicated functional modification of CQDs and any electron or energy transfer process [29]. Similar to FRET, IFE also depends on the spectral overlap between the fluorophore and the absorber. However, there is no distance requirements between the energy donor and the absorber in IFE [30]. IFE occurs when the absorption spectrum of the quencher in the detection system overlaps the excitation or emission spectrum of CQDs [31]. Therefore, the combination of CQDs and the fluorescence IFE mechanism will provide a new facile and low-cost strategy for sensitive fluorescence detection of OPs.

Herein, we designed a sensitive acephate detection method based on enzyme inhibition and the CQDs-mediated IFE effect. A detection strategy with fluorescence ratiometric response characteristics was developed using OPD and CQDs as indicators. In the presence of acephate, acephate acts as an inhibitor of AChE and blocks the production of thiocholine, which prevents the formation of Ag^+ metal-polymer, and further triggers the oxidation of OPD to produce yellow 2,3-diaminophenazine (DAP) with fluorescence emission at 558 nm. The fluorescence intensity of CQDs (460 nm) is quenched by the IFE process due to overlapped spectra of DAP, forming a typical

ratiometric response. This method is simple and sensitive, and has achieved a limit of detection of 0.052 ppb, three orders of magnitude lower than the maximum allowable limit of acephate. This fluorescence method based on CQDs-mediated IEF has been further validated by testing tap water and pear samples spiked with acephate, indicating high potential for facile and sensitive detections of OPs.

2. Experimental Section

2.1 Reagents and Instruments

CQDs (size 4.5 nm, 50 mg/mL) were purchased from Xingzi New Material Development Co., Ltd. Acephate and acetamiprid (100 μg/mL in methanol) were procured from Beijing Tanmo Quality Inspection Technology Co., Ltd. Thiram was purchased from Shanghai Titan Technology Co., Ltd. SDM and $CaCl_2$ were provided by Shanghai Aladdin Biochemical Technology Co., Ltd. OPD was obtained from Xinfan Biological Technology Co., Ltd. Silver nitrate was purchased from Kermel Chemical Reagent Co., Ltd. (Tianjin, China). A pesticide rapid detection kit was purchased from Dayuan Oasis Food Safety Co., Ltd. (Guangzhou, China), which included the substrate (acetylcholine, ATCh), the hydrolytic catalyst (acetylcholinesterase, AChE), and phosphate buffer (pH = 8.0, used for eluting methyl parathion residues in fruits and vegetables).

The UV-vis absorbance spectra were measured using a UV-3100 spectrometer (Shanghai Mapada Instrument Co., Ltd.). The FL emission and excitation spectra were obtained by a fluorescence spectrometer FluroMax-4 (HORIBA Scientific). Deionized water (specific resistivity 18.2 MΩ·cm) produced with a Barnstead EasyPure UV/UF compact water system (Dubuque, IA) was used to prepare all buffers/solutions throughout the experiments. Ag^+-Thiocholine complexes and CQDs were characterized by XPS (Figure S1) and high-resolution TEM (Figure S2), respectively.

2.2 Optimization of Ag^+ concentration

A series of Ag^+ solutions with different concentrations of 0, 17, 34, 68, 85, 170, 340,

510, 680, 850, 1020, 1190, 1360, 1530, 1700 μmol/L were prepared in brown centrifuge tubes. Afterward, 250 μg/mL CQDs and 25 mmol/L OPD were added to these centrifuge tubes. After mixing, the reaction was left in a brown centrifuge tube for 5 minutes. Subsequently, the reacted solution was transferred to a micro quartz cuvette (300 μL each) for fluorescence emission spectroscopy measurement with the excitation wavelength of 360 nm. Finally, the emission peaks of CQDs at 460nm and DAP at 558nm were recorded to calculate the ratiometric response I_{558}/I_{460}.

2.3 Quantitative detection of acephate

A series of different concentrations of acephate solutions were first prepared to establish calibration curves. 1 μL of AChE was mixed with 25 μL of each acephate solution with different concentrations and were left to react at room temperature for 25 minutes. Subsequently, 1 μL of ATCh was added and incubated in dark at 37°C for 15 minutes. After these incubation processes, a solution with 95 μL 700 μmol/L Ag^+, 283 μL 250 μg/mL CQDs and 95 μL 25 mmol/L OPD was added and mixed in the reaction system. After 5 minutes of reacting in each of the brown centrifuge tubes at 37 ℃ was complete, the fluorescence spectra were measured under 360 nm excitation. The fluorescence signals of CQDs at 460 nm (I_{460}) and DAP at 558 nm (I_{558}) were recorded, and the ratiometric fluorescence signal I_{558}/I_{460} was used for quantitative analysis of acephate.

2.4 Real samples preparation

Different concentrations of standard acephate (400, 200, 100, 40 ng/mL) were mixed with tap water from our laboratory faucets in a volume ratio of 1:1, and the final spiked concentrations were 200, 100, 50, and 20 ng/mL.

Fresh pears were purchased from the local supermarket and were washed thoroughly with ultrapure water. Pears were cut into five pieces. The samples (1.0 g each) were spiked with 0, 2000, 4000, 6000 and 8000 ng/mL acephate. The spiked samples were mixed with 5 mL of acetonitrile, extracted ultrasonically for 10 min, and centrifuged

for 10 min at 4000 rpm. 3.5 mL of the supernatant was extracted and filtered through anhydrous sodium sulfate, and the volume was adjusted to 5 mL for detection. The final spiked concentrations were 0, 23.33, 46.67, 70.00 and 93.33 ng/mL.

3. Results and discussion

3.1 Principle of the acephate detection system

The principle of ratiometric FL protocol is illustrated in Figure 1, in which the enzyme inhibition method is combined with the IFE to achieve the sensitive quantitation of acephate. When there is no acephate, AChE hydrolyzes ATCh to generate thiocholine[32], which combines with Ag^+ to form metal-polymers[33]. Hence, the fluorescence intensity of the reaction mainly comes from the emission of CQDs at 460nm. However, in the presence of acephate, which acts as an inhibitor of AChE, acephate will prevent the hydrolysis of ATCh from producing thiocholine, thereby preventing the formation of metal-polymers formed by thiocholine and Ag^+. Furthermore, the oxidation of OPD by Ag^+ is triggered to generate yellow DAP, which emits fluorescence at 558nm (excitation 360 nm) and quenches the fluorescence intensity of CQDs through IFE. By establishing the relationship curve between the concentration of acephate and I_{558}/I_{460}, the quantitative detection of acephate can be realized.

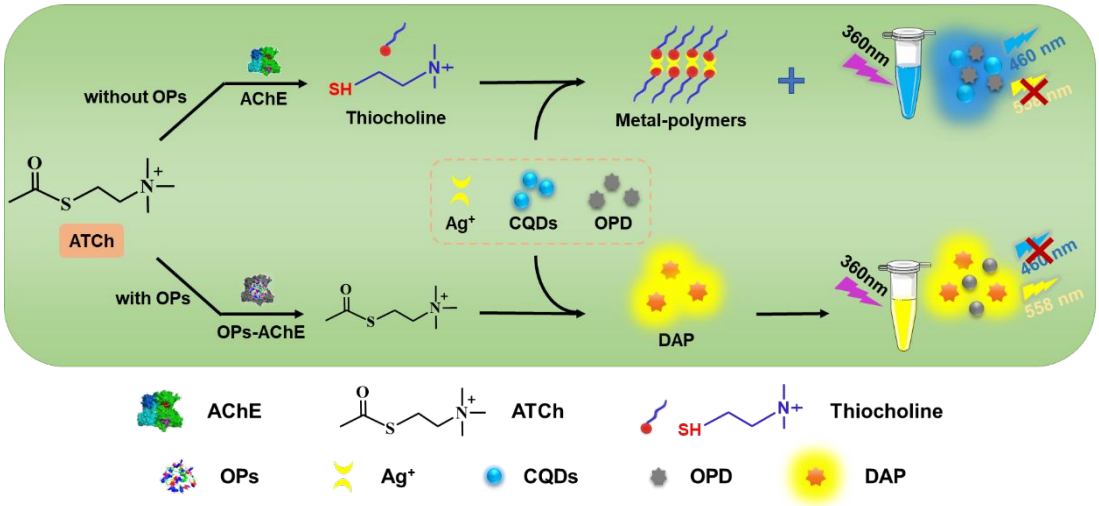

Figure 1. Schematic illustration of the principle of sensitive and quantitative detection of acephate based on CQDs-mediated IFE.

In this work, the IFE between CQDs and DAP is the key to the high-sensitivity quantification of acephate. Figure 2(a) shows the absorption spectra of OPD and DAP and the emission spectra of CQDs. It can be seen that there are large overlaps between the emission spectrum of CQDs and the absorption spectrum of DAP, which contributes to the generation of the IFE mechanism, and provides the feasibility for establishing the ratiometric responses of the fluorescence intensity of DAP and CQDs.

After establishing the aforementioned acephate detection system, the feasibility of the ratiometric system for sensitive detection of acephate was evaluated by testing OPD, Ag^+, ATCh, AChE, and OPs, respectively. As shown in Figure 2(b), when there were only CQDs and colorless OPDs in the system, only the characteristic emission peaks (black and red curve) of CQDs are displayed. Once Ag^+ was further added to the above system, the colorless OPD generated DAP due to the oxidation of Ag^+, which effectively quenched the fluorescence intensity of CQDs through the IFE mechanism, resulting in the appearance of double fluorescence peaks (green curve). When ATCh, AChE, or OPs were added to the system separately, because ATCh, AChE or OPs alone did not have an effect on the system, the peaks remained the same, including the characteristic peaks of CQDs and DAP. When ATCh and AChE were added at the same time, the hydrolysate of ATCh preferentially produced metal-polymers with Ag^+, and the oxidation of OPD was inhibited (purple line), leading to only one peak from CQDs. On the other hand, when OPs was added to the detection system, it irreversibly prevented the catalytic activity of AChE, leading to inhibition of ATCh hydrolysis. Therefore, the dual effects from the CQDs emitted fluorescence and the inhibitory effect from DAP (i.e., IFE) that was correlated to the concentration of OPs, form the ratiometric FL signal for quantitative detection of OPs, and the yellow line further confirmed its feasibility.

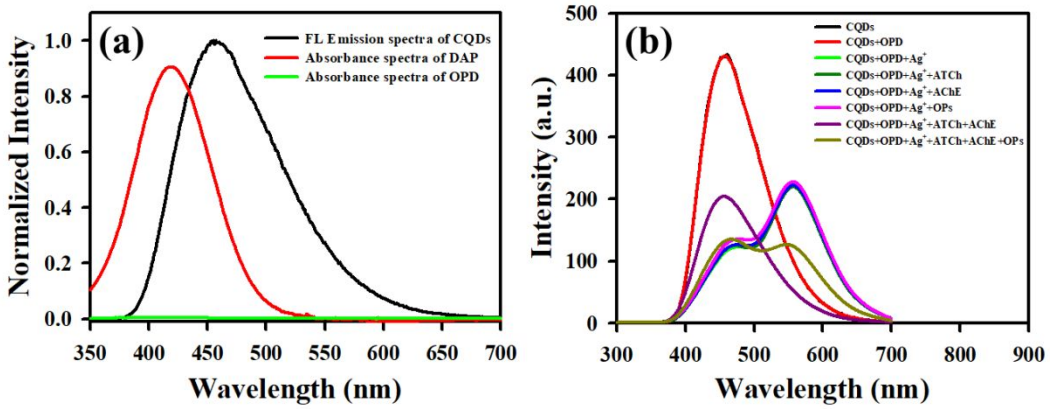

Figure 2. (a) UV-vis absorbance spectra of OPD and DAP, and the fluorescence spectra of CQDs. (b) Feasibility test of the ratiometric strategy.

3.2 Influences of Ag^+ and OPD on the fluorescence of CQDs

To verify that in the detection system the quenching of the fluorescence intensity of CQDs in the detection system is only caused by the change of Ag^+ concentrations due to the change of acephate concentrations, and OPD or Ag^+ itself will not affect the fluorescence intensity of CQDs. We separately studied the effects of adding different concentrations of Ag^+ and different concentrations of OPD on the fluorescence intensity of CQDs. 250 μg/mL CQDs was mixed with Ag^+ solutions at different concentrations (0, 100, 200, 300, 400, 500 μmol/L) at a volume ratio of 1:1. Excited under 360 nm light, the measured fluorescence intensities of CQDs with different concentrations of Ag^+ at 460 nm are shown in Figure 3(a). With the addition of different concentrations of Ag^+, the fluorescence intensity of CQDs remained almost unchanged.

In addition, we explored the influence of different concentrations of OPD on the fluorescence intensity of CQDs. After mixing 250 μg/mL CQDs with different concentrations (0, 2.0, 4.0, 6.0, 8.0, 10.0 mmol/L) of OPD (volume ratio 1:1), the fluorescence intensity was measured and shown in Figure 3(b). With the addition of different concentrations of OPD, the fluorescence intensity of CQDs also remained virtually unchanged. Thus, the above experimental results confirmed that the addition of Ag^+ or OPD alone does not cause the fluorescence quenching of CQDs.

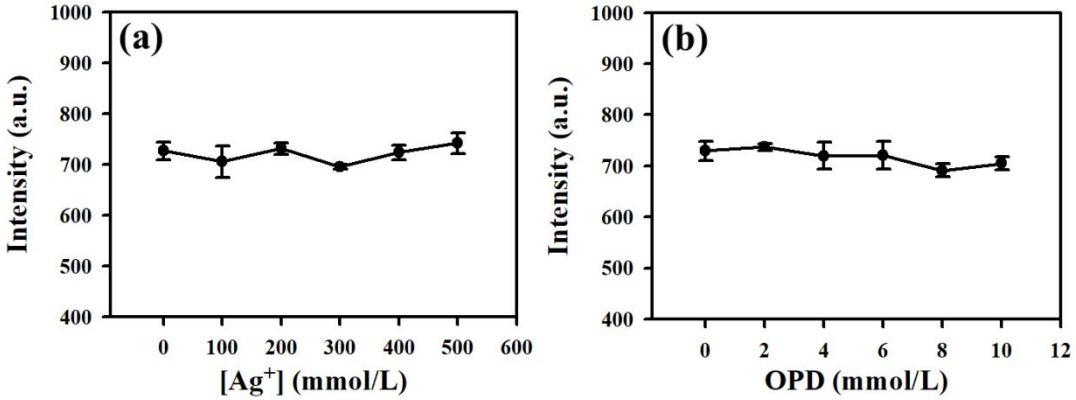

Figure 3. The effect of Ag^+ (a) and OPD (b) on CQDs fluorescence intensity.

3.3 Optimization of Ag^+ concentration

To confirm the IFE effect between CQDs and DAP, different Ag^+ concentrations (0-1000 μmol/L) were added to the system and were left to react for 5 minutes. We can see from Figure 4(a) that as the Ag^+ concentration increased, the fluorescence intensity of CQDs at 460 nm gradually decreased, while the emission intensity of DAP at 558 nm gradually increased, which further verified the IFE effect between CQDs and DAP. Figure 4(b) shows the trend of the fluorescence intensity at 558 nm with the change of the Ag^+ concentration. The fluorescence at 558 nm from DAP gradually increased with the increase of the Ag^+ concentrations. When the Ag^+ concentration was 700 μmol/L, the DAP fluorescence enhancement at 558 nm reached saturation. Therefore, the final concentration of Ag^+ was chosen to be 700 μmol/L for the optimal detection of acephate in the subsequent experiments.

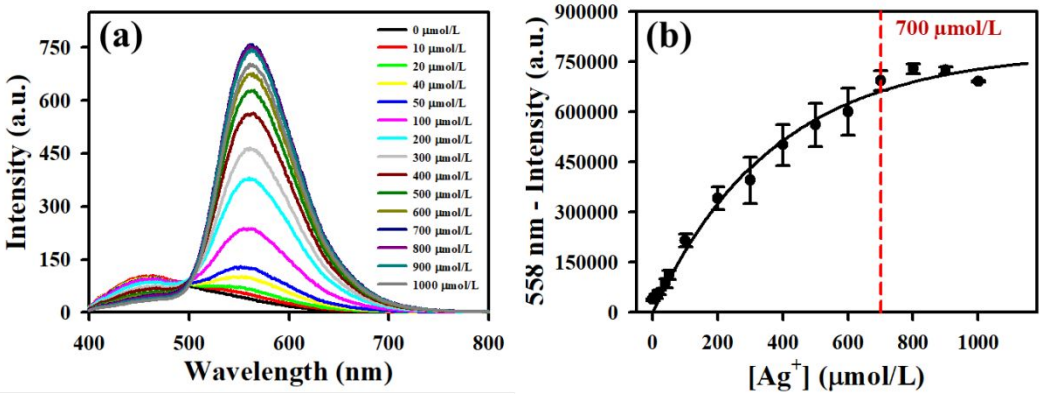

Figure 4. Optimization of the concentrations of Ag^+. (a) Fluorescence spectra caused by different concentrations of Ag^+. (b) The fluorescence intensity at 558 nm with the change of the Ag^+

concentration. When the concentration of Ag^+ wasd 700 μmol/L, the fluorescence enhancement of the DAP was saturated.

3.4 Quantitative detection of acephate based on enzyme inhibition combined with IFE effects

After condition optimization, we have tested various concentrations of acephate using the biosensor based on enzyme inhibition and CQDs-mediated fluorescence internal filtration effect. Figure 5(a) shows the fluorescence spectra measured by a fluorescence spectrometer under excitation of 360 nm, with different concentrations of acephate ranging from 0 to 100 ng/mL. It can be seen that with the increase in the concentration of acephate, the fluorescence intensity (460 nm) of CQDs gradually weakened, while the fluorescence intensity (558 nm) of DAP gradually increased. A good linear relationship (R^2=0.981) between the ratiometric response (I_{558}/I_{460}) and the logarithm of the concentration of acephate was obtained over the range from 0 to 100 ng/mL in Figure 5(b). The regression equation was y = 0.3098 (±0.0225) $\log_{10}$X + 0.7677 (± 0.0320), where X was the concentration of acephate and y was the fluorescent ratiometric signal I_{558}/I_{460}. According to the 3σ principle (signal-to-noise ratio of 3), the detection limit of this detection method was calculated to be 0.052 ppb. Compared with other OPs detection methods, as listed in Table 1, our detection system has a much lower detection limit and wider linear range (Table 1). Our LOD is at least 40 times lower than (compared to 2 ppb) those of other methods.

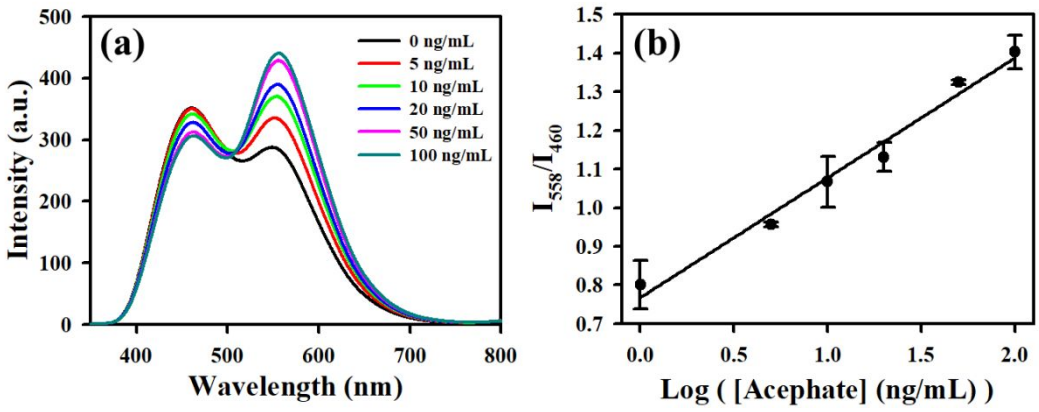

Figure 5. (a) Fluorescence spectra of concentrations of acephate (0, 5, 10, 20, 50 and 100 ng/mL) measured by the biosensor based on enzyme inhibition combined with IFE effects. (b) Linear plot

of ratiometric response I_{558}/I_{460} versus the logarithm of the concentration of acephate.

Table 1. Comparison with other detection methods for OPs.

Sensing Method	Liner Range	LOD	Ref.
Colorimetric Enzymatic Inhibition	10-500 nM	10 nM	[17]
Electrochemical	2-20 ppb	2 ppb	[13]
Fluorescence	0.015-1.5 mM	24.7 ng/mL	[26]
Surface-Enhanced Raman	0.5-100.2 mg/L	0.5 mg/L	[20]
GC-MS/MS	16-100 ppb	5 ppb	[34]
IFE Fluorescence	0-100 ng/mL	0.052 ppb	This work

3.5 Acephate detection in real samples

From the perspective of real applications, it is crucial to evaluate the method by testing acephate residues in food products and environmental samples. In this work, the application of this detection method was demonstrated by testing spiked acephate in tap water and pear samples.

Tap water was spiked with different concentrations of acephate (20, 50, 100 and 200 ng/mL) using the standard addition method. Figure 6 (a) shows the fluorescence spectrum under the 360 nm excitation after adding 20, 50, 100, and 200 ng/mL acephate to tap water. To study the accuracy of the detection system, we conducted a recovery test using the standard addition method. As shown in Table 2, the recovery rates of acephate with known spiked samples were measured in the range of 95~106.65% for tap water samples, and a relative standard deviation (RSD) of less than 1.28% was obtained, indicating good accuracy and high reproducibility of our method.

The method was further validated by testing pear samples. Pear samples were prepared according to the “Real samples preparation” section, in which the spiked concentrations were 0, 23.33, 46.67, 70.00, and 93.33 ng/mL. Figure 6 (b) shows the fluorescence spectra of different concentrations of spiked acephate in pear samples. As listed in Table 3, the recoveries for the known spiked pear samples of acephate were determined

to be in the range of 93.51~111.15%, which met the criterion on quality control of laboratories-chemical testing of food.

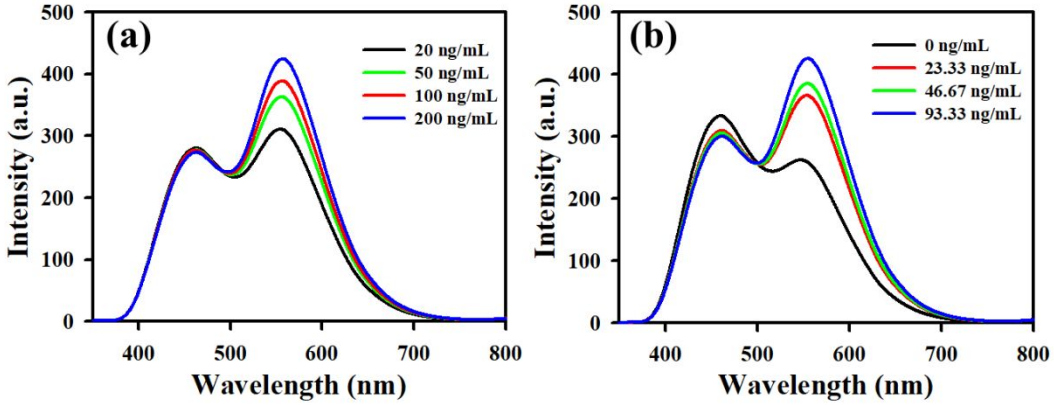

Figure 6. (a) Fluorescence spectra of the system by spiking varied concentrations of acephate in tap water (20, 50, 100 and 200 ng/mL). (b) Fluorescence spectra of the system by spiking varied concentrations of acephate in pear (0, 23.33, 46.67, and 93.33 ng/mL).

Table 2. Determination of Acephate in Tap water Samples.

Sample	Added Value (ng/mL)	Found (ng/mL)	Recovery (n=3, %)	RSD (n=3, %)
Tap Water	0	/	/	/
	20	21.33	106.65	1.28
	50	47.89	95.78	1.03
	100	106.09	106.09	0.98
	200	202.30	101.15	1.17

Table 3. Determination Results of Acephate in Pear Samples.

Sample	Added Value (ng/mL)	Found (ng/mL)	Recovery (n=3, %)	RSD (n=3, %)
Pear	0	/	/	/
	23.33	25.93	111.15	4.17
	46.67	43.64	93.51	3.87
	93.33	98.60	105.64	4.23

3.6 Selectivity of the detection system

To evaluate the selectivity of the detection system, 1000 ng/mL of other interfering substances (acetamiprid, thiram, sulfa antibiotics (SDM), and Ca^{2+}) were chosen to

investigate the anti-interference ability of our method, while the concentration of acephate was kept at 100 ng/mL. As shown in Figure 7, the signal intensity ratio I_{558}/I_{460} of acephate was the highest, reaching 1.43, whereas the ratiometric signals I_{558}/I_{460} of other interfering substances were similar to the blank and much lower than the signal caused by acephate, though high concentrations of interfering substances were used. These results indicated that the detection system has high selectivity for organophosphorus pesticides.

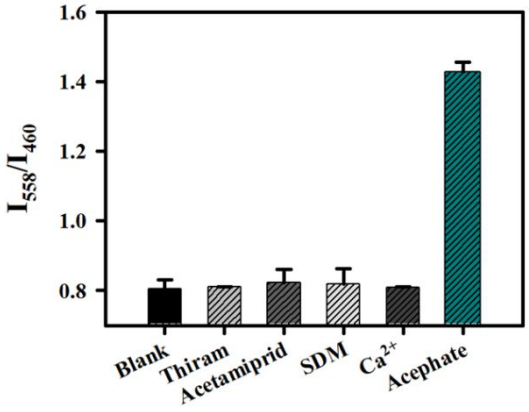

Figure 7. Selectivity investigation. Acephate, 100 ng/mL; other interfering agents, 1000 ng/mL.

4. Conclusion

In summary, a new enzyme inhibition method combined with the IFE effect has been developed for the sensitive quantitative detection of acephate. The dual effects from the CQDs emitted fluorescence and the inhibitory effect from DAP (i.e., IFE) that was correlated to the concentration of OPs form the ratiometric fluorescence response, which was used for quantitative detection of OPs. The detection limit of this method is 0.052 ppb, which is far lower than the standards for acephate from China and EU in food safety administration (e.g., 0.02 ppm for China). Compared with traditional enzyme inhibition methods, this method exhibits much higher detection sensitivity. Leveraging a portable fluorescence detector and an integrated microfluidic device to be developed [35-38], this method will have great potential for rapid and ultrasensitive screening of trace pesticide residues on site, and broad application in food safety testing, environmental pollution monitoring, and poisoning estimation.

Author contributions

Haiqin Li: conceptualization, methodology, formal analysis, investigation, validation, data curation, writing - original draft, writing - review and editing. Rong Deng: conceptualization, methodology, formal analysis. Hamed Tavakoli: writing - review and editing. Xiaochun Li: Project administration, conceptualization, formal analysis, supervision, funding acquisition, methodology, resources, writing - review and editing. XiuJun Li: formal analysis, conceptualization, methodology, resources, writing - review and editing.

Declaration of Competing Interest

The authors declare the following competing financial interest(s). The authors from TYUT have filed a China Patent Application (No. 202110392652. 4) to protect the IP associated with the technology described in this paper. Other authors declare no competing interest.

ACKNOWLEDGMENTS

We gratefully acknowledge the financial support from the Natural Science Foundation of China (grant no. 21874098), Shanxi Province International Collaboration Project (grant no. 201903D421053), and University Scientific and Technological Transformation and Cultivation Project of Shanxi province. We are also grateful to the support from the U.S. CPRIT (RP210165), the U.S. NSF (IIP2122712, IIP2052347, and CHE2216473), NIH/NIAID (R41AI162477), and the U.S. DOT (CARTEEH).

Reference

[1] S. V. Boxstael, I. Habib, L. Jacxsens, M. D. Vocht, L. Baert, E. V. de Perre, A. Rajkovic, F. Lopez-Galvez, I. Sampers, P. Spanoghe, B. D. Meulenaer and M. Uyttendaele, Food safety issues in fresh produce: bacterial pathogens, viruses and pesticide residues indicated as major concerns by stakeholders in the fresh produce chain, Food Control, 2013, 32,190-197.

[2] G.T. Bakirci, D.B.Y. Acay, F. Bakirci and S. Otles, Pesticide residues in fruits and vegetables from the Aegean region, Turkey, Food Chem., 2014, 160, 379-392.

[3] L. Wan, Y. Wu, H. Ding and W. Zhang, Toxicity, Biodegradation, and Metabolic Fate of Organophosphorus Pesticide Trichlorfon on the Freshwater Algae Chlamydomonas reinhardtii, J. Agr. Food Chem., 2020, 68, 1645-1653.

[4] J. R. Richardson, H. W. Chambers and J. E. Chambers, Analysis of the additivity of in vitro inhibition of cholinesterase by mixtures of chlorpyrifos-oxon and azinphos-methyl-oxon, Toxicol. Appl. Pharm., 2001, 172, 128-139.

[5] M. Eddleston, N. A Buckley, P. Eyer and Andrew H Dawson, Management of acute organophosphorus pesticide poisoning, The Lancet, 2008,371, 597-607.

[6] https://www.who.int/news-room/fact-sheets/detail/pesticide-residues-in-food.

[7] C.R. Bojaca, L.A. Arias, D.A. Ahumada, H.A. Casilimas and E. Schrevens, Evaluation of pesticide residues in open field and greenhouse tomatoes from Colombia, Food Control, 2013, 30, 400-403.

[8] P. Pugliese, J.C. Molto´, P. Damiani, R. Mar´ın, L. Cossignani and J. Manes, Gas chromatographic evaluation of pesticide residue contents in nectarines after non-toxic washing treatments, J. Chromatogr. A, 2004, 1050, 185-191.

[9] X. Mao, A. Yan, Y.Wan, D. Luo and H. Yang, Dispersive Solid-Phase Extraction Using Microporous Sorbent UiO-66 Coupled to Gas Chromatography-Tandem Mass Spectrometry: A QuEChERS-Type Method for the Determination of Organophosphorus Pesticide Residues in Edible Vegetable Oils without Matrix Interference, J. Agr. Food Chem., 2019, 67, 1760-1770

[10] K. Seebunrueng, Y. Santaladchaiyakit and S. Srijaranai, Vortex-assisted low-density solvent based demulsified dispersive liquid-liquid microextraction and high-performance liquid chromatography for the determination of OP in water samples, Chemosphere, 2014, 103, 51-58.

[11] C. García-Ruiz, G Álvarez-Llamas, Á. Puerta, E. Blanco, A. Sanz-Medel and M. Marina,

Enantiomeric separation of OP by capillary electrophoresis: Application to the determination of malathion in water samples after preconcentration by off-line solid-phase extraction, Anal. Chim. Acta, 2005, 543, 77-83.

[12] J. Yao, Z. Wang, L. Guo, X. Xu, L. Liu, L. Xu, S. Song, C. Xu and H. Kuang, Advances in immunoassays for organophosphorus and pyrethroid pesticides, Trac-Trend Anal. Chem., 2020, 131,116022.

[13] F. Arduinia, S. Cinti, V. Caratelli, L. Amendola, G. Palleschi and D. Moscone, Origami multiple paper-based electrochemical biosensors for pesticide detection, Biosens. Bioelectron., 2019, 126, 346-354.

[14] X. Xie, B. Zhou, Y. Zhang, G. Zhao and B. Zhao, A multi-residue electrochemical biosensor based on graphene/chitosan/parathion for sensitive OP detection, Chem. Phys. Lett., 2021, 767, 138355.

[15] J. Guo, J. X. H. Wong, C. Cui, X. Li and H.-Z. Yu, A smartphone-readable barcode assay for the detection and quantitation of pesticide residues, Analyst, 2015, 140, 5518-5525.

[16] X. Meng, C. W. Schultz, C. Cui, X. Li and H.-Z. Yua, On-site chip-based colorimetric quantitation of OP using an office scanner, Sens. Actuators B Chem., 2015, 215, 577-583.

[17] I. Jang, D. B. Carrão, R. F. Menger, A. R. M. de Oliveira and C. S. Henry, Pump-Free microfluidic rapid mixer combined with a paper-based channel, ACS Sensors, 2020, 5, 2230-2238.

[18] A. V. Alex and A. Mukherjee, Review of recent developments (2018-2020) on ATChsterase inhibition-based biosensors for OP detection, Microchem. J., 2021, 161, 105779.

[19] M. Zhang, J. Yang, Y. Wang, H. Sun, H. Zhou, X. Liu, C. Ye, Z. Bao, J. Liu and Y. Wu, Plasmon-coupled 3D porous hotspot architecture for super-sensitive quantitative SERS sensing of toxic substances on real sample surfaces, Phys. Chem. Chem. Phys., 2019, 21, 19288-19297.

[20] S. Weng, W. Zhu, P. Li, H. Yuan, X. Zhang, L. Zheng, J. Zhao, L. Huang and P. Han, Dynamic surface-enhanced Raman spectroscopy for the detection of acephate residue in rice by using gold nanorods modified with cysteamine and multivariant methods, Food Chem., 2020, 310, 125855.

[21] H. Tavakoli, W. Zhou, L. Ma, S. Perez, A. Ibarra, F. Xu, S. Zhan and X. Li, Recent advances in microfluidic platforms for single-cell analysis in cancer biology, diagnosis and therapy, TRAC - Trend Anal. Chem., 2019, 117, 13-26.

[22] M. Lv, W. Zhou, H. Tavakoli, C. Bautista, J. Xia, Z. Wang and X. Li, Aptamer-functionalized

Metal-organic frameworks (MOFs) for biosensing, Biosens. Bioelectron., 2021, 176, 112947.

[23] R. Jin, D. Kong, X. Yan, X. Zhao, H. Li, F. Liu, P. Sun, Y. Lin and G. Lu, Integrating Target-Responsive Hydrogels with Smartphone for On-Site ppb-Level Quantitation of Organophosphate Pesticides, ACS Appl. Mater. Inter., 2019, 11, 27605-27614.

[24] Q. Wang, Q. Yin, Y. Fan, L. Zhang, Y. Xu, O. Hu, X. Guo, Q. Shi, H. Fu and Y. She, Double quantum dots-nanoporphyrin fluorescence-visualized paper-based sensors for detecting OP, Talanta, 2019, 199, 46-53.

[25] M. Jiang, C. Chen, J. He, H. Zhang and Z. Xu, Fluorescence assay for three OP in agricultural products based on Magnetic-Assisted fluorescence labeling aptamer probe, Food Chem., 2020,307, 125534.

[26] J. Wang, J. Zhang, J. Wang, G. Fang, J. Liu and S. Wang, Fluorescent peptide probes for organophosphorus pesticides detection, J. Hazard. Mater., 2020, 389, 122074.

[27] S. Zhu, Q. Meng, L. Wang, J. Zhang, Y. Song, H. Jin, K. Zhang, H. Sun, H. Wang and B. Yang, Highly photoluminescent carbon dots for multicolor patterning, sensors, and bioimaging, Angew. Chemie - Int. Ed., 2013, 52, 3953-3957.

[28] S.Y. Lim, W. Shen and Z. Gao, Carbon quantum dots and their applications, Chem. Soc. Rev., 2015, 44 , 362-381.

[29] S. Lu, G. Li, Z. Lv, N. Qiu, W. Kong, P. Gong, G. Chen, L. Xia, X. Guo, J. You, Y. Wu, Facile and ultrasensitive fluorescence sensor platform for tumor invasive biomaker beta-glucuronidase detection and inhibitor evaluation with carbon quantum dots based on inner-filter effect, Biosens. Bioelectron., 2016, 85, 358-362.

[30] X. Li, S. Zhao, B. Li, K. Yang, M. Lan, L. Zeng, Advances and perspectives in carbon dot-based fluorescent probes: Mechanism, and application, Coordin. Chem. Rev., 2021, 431, 213686.

[31] J. Wang, Q. Liu, Y. Liang and G. Jiang, Recent progress in application of carbon nanomaterials in laser desorption/ionization mass spectrometry, Anal. Bioanal. Chem., 2016, 408, 2861-2873.

[32] B.G. Katzung, Basic and clinical pharmacology:Introduction to autonomic pharmacology (8 ed.). The McGraw Hill Companies. 2001, pp. 75-91. ISBN 978-0-07-160405-5.

[33] J. Zhang, W. Zheng and X. Jiang, Ag^{+}-Gated Surface Chemistry of Gold Nanoparticles and Colorimetric Detection of Acetylcholinesterase, Small, 2018, 14, 1801680.

[34] X. Zhao, W.n Kong, J. Wei and M. Yang, Gas chromatography with flame photometric

detection of 31organophosphorus pesticide residues in Alpinia oxyphylla dried fruits, Food Chem., 2014, 162, 270-276.

[35] W. Zhou, M. Dou, S. S. Timilsina, F. Xu and X. Li, Recent innovations in cost-effective polymer and paper hybrid microfluidic devices, Lab Chip, 2021, 21, 2658-2683.

[36] M. Dou, S. T. Sanjay, M. Benhabib, F. Xu and X. Li, Low-cost Bioanalysis on Paper-based & Its Hybrid Microfluidic Platforms, Talanta, 2015, 145, 43-54.

[37] M. Dou, N. Macias, F. Shen, J. D. Bard, D. C. Domínguez and X. Li, Rapid and Accurate Diagnosis of the Respiratory Disease Pertussis on a Point-of-Care Biochip, EClinicalMedicine, 2019, 8, 72-77.

[38] K. S. Prasad, X. Cao, N. Gao, Q. Jin, S. T. Sanjay, G. Henao-Pabon and X. Li, A Low-Cost Nanomaterial-based Electrochemical Immunosensor on Paper for High-sensitivity Early Detection of Pancreatic Cancer, Sens. Actuators B Chem., 2020, 305, 127516.